

# Discrimination of Supersymmetry and Universal Extra Dimensions at Hadron Colliders

AseshKrishna Datta

*MCTP, University of Michigan, Ann Arbor, MI 48109-1120, USA*

Kyoungchul Kong and Konstantin T. Matchev

*Institute for Fundamental Theory, Physics Department,*

*University of Florida, Gainesville, FL 32611, USA*

(Dated: September 22, 2005)

## Abstract

We contrast the experimental signatures of low energy supersymmetry and the model of Universal Extra Dimensions and discuss various methods for their discrimination at hadron colliders. We study the discovery reach of the Tevatron and the LHC for level 2 Kaluza-Klein modes, which would indicate the presence of extra dimensions. We find that with  $100 \text{ fb}^{-1}$  of data the LHC will be able to discover the  $\gamma_2$  and  $Z_2$  KK modes as separate resonances if their masses are below 2 TeV. We also investigate the possibility to differentiate the spins of the superpartners and KK modes by means of the asymmetry method of Barr.

PACS numbers: 11.10.Kk,12.60.Jv,14.80.Ly

## I. INTRODUCTION

With the highly anticipated run of the Large Hadron Collider (LHC) at CERN we will begin to explore the Terascale in earnest. There are very sound reasons to expect momentous discoveries at the LHC. Among the greatest mysteries in particle physics today is the origin of electroweak symmetry breaking, which, according to the Standard Model, is accomplished through the Higgs mechanism. The Higgs particle is the primary target of the LHC experiments and, barring some unexpected behavior, the Higgs boson will be firmly discovered after only a few years of running of the LHC. With some luck, a Higgs signal might start appearing already in the Tevatron Run II.

The discovery of a Higgs boson, however, will open a host of new questions. As the first fundamental scalar to be seen, it will bring about a worrisome fine tuning problem: why is the Higgs particle so light, compared to, say, the Planck scale? Various solutions to this hierarchy problem have been proposed, and the most aesthetically pleasing one at this point appears to be low energy supersymmetry (SUSY). In SUSY, the problematic quadratic divergences in the radiative corrections to the Higgs mass are absent, being canceled by loops with superpartners. The cancellations are enforced by the symmetry, and the Higgs mass is therefore naturally related to the mass scale of the superpartners.

While the solution of the hierarchy problem is perhaps the most celebrated virtue of SUSY, supersymmetric models have other side benefits. For one, if the superpartners are indeed within the TeV range, they would modify the running of the gauge couplings at higher scales, and gauge coupling unification takes place with astonishing precision. Secondly, a large class of SUSY models, which have a conserved discrete symmetry ( $R$ -parity), contain an excellent dark matter candidate: the lightest neutralino  $\tilde{\chi}_1^0$ . One should keep in mind that the dark matter problem is by far the most compelling *experimental* evidence for particles and interactions outside the Standard Model (SM), and provides a completely independent motivation for entertaining supersymmetry at the TeV scale. Finally,  $R$ -parity implies that superpartners interact only pairwise with SM particles, which guarantees that the supersymmetric contributions to low energy precision data only appear at the loop level and are small. In summary, supersymmetric extensions of the SM are the primary candidates for new physics at the TeV scale. Not surprisingly, therefore, the signatures of supersymmetry at the Tevatron and LHC have been extensively discussed in the literature. In typical

scenarios with superpartners in the range of a few TeV or less, already within the first few years of running the LHC will discover a signal of new physics in several channels. Once such a signal of physics beyond the Standard Model is seen, it will immediately bring up the question: is it supersymmetry or not?

The answer to this question can be approached in two different ways. On the theoretical side, one may ask whether there are well motivated alternatives to low energy supersymmetry, which would give similar signatures at hadron colliders, in other words, if the new physics is not supersymmetry, what else can it be? Until recently, there were no known examples of other types of new physics, which could “fake” supersymmetry sufficiently well. The signatures of supersymmetry and its competitors (technicolor, new gauge bosons, large extra dimensions, etc.) were sufficiently distinctive, and there was little room for confusion. However, it was recently realized that the framework of Universal Extra Dimensions (UED), originally proposed in [1], can very effectively masquerade as low energy supersymmetry at a hadron collider such as the LHC or the Tevatron [2]. It therefore became of sufficient interest to try and prove supersymmetry at the LHC from first principles, without resorting to model-dependent assumptions and without theoretical bias. The experimental program for proving supersymmetry at a *lepton* collider has been outlined a long time ago [3] and can be readily followed to make the discrimination between SUSY and UED [4, 5, 6, 7]. However, as we shall see below, the case of hadron colliders is much more challenging.

The more direct approach to confirming supersymmetry at the LHC would be to first ask: what are the defining features of supersymmetry, and can we prove them from the data? By now there is a wide variety of supersymmetric models, with very diverse phenomenology. Nevertheless, they all share the following common features which define a supersymmetric framework:

1. For each particle of the Standard Model, supersymmetry predicts a new particle (superpartner).
2. The spins of the superpartners differ by  $1/2$  unit.
3. The couplings of the particles and their superpartners are equal, being related by supersymmetry.

If supersymmetry were exact, one would have another common feature: the prediction that the masses of the particles and their superpartners must be equal as well. However, once

SUSY is broken (as it must be), the superpartner masses are lifted and one obtains spectra classified by the mechanism of SUSY breaking: supergravity-mediated, gauge-mediated, gaugino-mediated, anomaly-mediated etc. (for a recent review, see [8]). As a result, in realistic models of low-energy supersymmetry the pattern of sparticle masses is very model-dependent. The measurements of the superpartner masses are therefore probing SUSY *breaking* phenomena rather than a fundamental property of supersymmetry itself.

In the following let us only concentrate on SUSY models which possess a weakly interacting massive particle (WIMP) as a dark matter candidate, as guaranteed by  $R$ -parity conservation. This will be in fact the most difficult case for establishing supersymmetry at a hadron collider. Due to  $R$ -parity, the superpartners are pair-produced, and each one decays to the lightest supersymmetric particle (LSP), in this case  $\tilde{\chi}_1^0$ . Since the two  $\tilde{\chi}_1^0$ s leave the detector without any interaction, the generic SUSY signal at the LHC is missing energy. With these assumptions, we can add another identifying feature to the list above, although this is not required by supersymmetry itself:

4. The generic collider signature of supersymmetric models with WIMP LSPs is missing energy.

This last property makes exact reconstruction of the event kinematics practically impossible. At a hadron collider, the center of mass energy is not known on an event per event basis. In addition, the momenta of *both*  $\tilde{\chi}_1^0$  particles are unknown, and what is measured is only the transverse component of the sum of their momenta, provided there are no other sources of missing energy in the event (such as neutrinos,  $b$ -jets,  $\tau$ -jets, etc.). As we shall see below, this incomplete information is the main stumbling block in proving the basic properties of supersymmetry at the LHC.

The purpose of this paper is to investigate the prospects for establishing supersymmetry at the LHC by discriminating it from its look-alike scenario of Universal Extra Dimensions. In Section II we review the basic phenomenology of the UED model, contrasting it with a generic supersymmetric model as described above. We identify two basic discriminators between the two scenarios and proceed to consider each one in turn in the following two sections. One of the characteristic features of extra dimensional models is the presence of a whole tower of Kaluza-Klein (KK) partners, labelled by their KK level  $n$ . In contrast,  $N = 1$  supersymmetry predicts a single superpartner for each SM particle. One might

therefore hope to discover the higher KK modes of UED and thus prove the existence of extra dimensions. In Section III we study the discovery reach for level 2 KK gauge boson particles and the resolving power of the LHC to see them as separate resonances. The other fundamental difference between SUSY and UED is the spin of the superpartners (KK partners). In Section IV we study how well the two models can be distinguished based on spin correlations in the cascade decays of the new particles. In particular, we use the asymmetry variable recently advertised by Barr [9] for this purpose<sup>1</sup>. We present our conclusions in Section V.

## II. PHENOMENOLOGY OF UNIVERSAL EXTRA DIMENSIONS

### A. The Minimal UED Model

Models of UED place all Standard Model particles in the bulk of one or more compactified extra dimensions. In the simplest and most popular version, there is a single extra dimension of size  $R$ , compactified on an  $S_1/Z_2$  orbifold [1]. More complicated 6-dimensional models have also been built [15, 16]. The UED framework has been a fruitful playground for addressing different puzzles of the Standard Model, such as electroweak symmetry breaking and vacuum stability [17, 18, 19], neutrino masses [20, 21], proton stability [22] or the number of generations [23]. A peculiar feature of UED is the conservation of Kaluza-Klein number at tree level, which is a simple consequence of momentum conservation along the extra dimension. However, bulk and brane radiative effects [24, 25, 26] break KK number down to a discrete conserved quantity, the so called KK parity,  $(-1)^n$ , where  $n$  is the KK level. KK parity ensures that the lightest KK partners (those at level one) are always pair-produced in collider experiments, just like in the  $R$ -parity conserving supersymmetry models discussed in Section I. KK parity conservation also implies that the contributions to various low-energy observables [27, 28, 29, 30, 31, 32, 33, 34, 35, 36, 37] only arise at loop level and are small. As a result, the limits on the scale  $R^{-1}$  of the extra dimension from precision electroweak data are rather weak, constraining  $R^{-1}$  to be larger than approximately 250 GeV [31]. An attractive feature of UED models with KK parity is the presence of a stable massive particle

---

<sup>1</sup> While this work was in preparation [10, 11, 12, 13], a similar study of the asymmetry was published in [14], with very similar conclusions, see Section IV.

which can be a cold dark matter candidate [26, 38]. The lightest KK partner (LKP) at level one is also the lightest particle with negative KK parity and is stable on cosmological scales. The identity of the LKP is a delicate issue, however, as it depends on the interplay between the one-loop radiative corrections to the KK mass spectrum and the brane terms generated by unknown physics at high scales [26]. In the minimal UED model defined below, the LKP turns out to be the KK partner  $B_1$  of the hypercharge gauge boson [26] and its relic density is typically in the right ballpark: in order to explain all of the dark matter, the  $B_1$  mass should be in the range 500-600 GeV [39, 40, 41, 42, 43, 44]. Kaluza-Klein dark matter offers excellent prospects for direct [45, 46, 47] or indirect detection [45, 48, 49, 50, 51, 52, 53, 54, 55, 56]. Once the radiative corrections to the Kaluza-Klein masses are properly taken into account, the collider phenomenology of the Minimal UED model exhibits striking similarities to supersymmetry [2, 57] and represents an interesting and well motivated counterexample which can “fake” supersymmetry signals at the LHC.

For the purposes of our study we have chosen to work with the minimal UED model considered in [2]. In UED the bulk interactions of the KK modes are fixed by the SM Lagrangian and contain no unknown parameters other than the mass,  $m_h$ , of the SM Higgs boson. In contrast, the boundary interactions, which are localized on the orbifold fixed points, are in principle arbitrary, and their coefficients represent new free parameters in the theory. Since the boundary terms are renormalized by bulk interactions, they are scale dependent [24] and cannot be completely ignored since they will be generated by renormalization effects. Therefore, one needs an ansatz for their values at a particular scale. Like any higher dimensional Kaluza-Klein theory, the UED model should be treated only as an effective theory valid up to some high scale  $\Lambda$ , at which it matches to some more fundamental theory. The Minimal UED model is then defined so that the coefficients of all boundary interactions vanish at this matching scale  $\Lambda$ , but are subsequently generated through RGE evolution to lower scales. The Minimal UED model therefore has only two input parameters: the size of the extra dimension,  $R$ , and the cutoff scale,  $\Lambda$ . The number of KK levels present in the effective theory is simply  $\Lambda R$  and may vary between a few and  $\sim 40$ , where the upper limit comes from the breakdown of perturbativity already below the scale  $\Lambda$ . Unless specified otherwise, for our numerical results below, we shall always choose the value of  $\Lambda$  so that  $\Lambda R = 20$ . Changing the value of  $\Lambda$  will have very little impact on our results since the  $\Lambda$  dependence of the KK mass spectrum is only logarithmic.

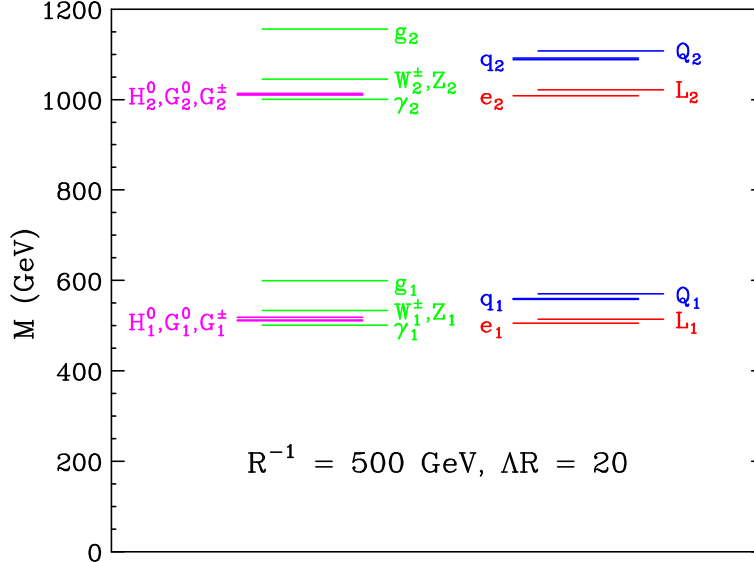


FIG. 1: One-loop corrected mass spectrum of the  $n = 1$  and  $n = 2$  KK levels in Minimal UED, for  $R^{-1} = 500 \text{ GeV}$ ,  $\Lambda R = 20$  and  $m_h = 120 \text{ GeV}$ . We show the KK modes of gauge bosons, Higgs and Goldstone bosons and first generation fermions.

In Fig. 1 we show the mass spectrum of the  $n = 1$  and  $n = 2$  KK levels in Minimal UED, for  $R^{-1} = 500 \text{ GeV}$ ,  $\Lambda R = 20$  and SM Higgs boson mass  $m_h = 120 \text{ GeV}$ . We include the full one-loop corrections from [26]. We have used RGE improved couplings to compute the radiative corrections to the KK masses. It is well known that in UED the KK modes modify the running of the coupling constants at higher scales. We extrapolate the gauge coupling constants to the scale of the  $n = 1$  and  $n = 2$  KK modes, using the appropriate  $\beta$  functions dictated by the particle spectrum [38, 58, 59]. As a result the spectrum shown in Fig. 1 differs slightly from the one in [26]. Most notably, the colored KK particles are somewhat lighter, due to a reduced value of the strong coupling constant, and overall the KK spectrum at each level is more degenerate.

## B. Comparison of UED and Supersymmetry

We are now in a position to compare in general terms the phenomenology of UED and supersymmetry at colliders. In Section I we outlined four identifying features of SUSY models with WIMP LSPs. In complete analogy, the discussion of Section II A leads to the following generic features of UED:

1. For each particle of the Standard Model, UED models predict an infinite<sup>2</sup> tower of new particles (Kaluza-Klein partners).
2. The spins of the SM particles and their KK partners are the same.
3. The couplings of the SM particles and their KK partners are equal.
4. The generic collider signature of UED models with WIMP LKPs is missing energy.

Notice that the defining features 3 and 4 are common to both supersymmetry and UED and cannot be used to distinguish the two cases. We see that while  $R$ -parity conserving SUSY implies a missing energy signal, the reverse is not true: a missing energy signal would appear in any model with a dark matter candidate, and even in models which have nothing to do with the dark matter issue, but simply contain new neutral quasi-stable particles, e.g. gravitons [60, 61, 62]. Similarly, the equality of the couplings (feature No. 3) is a celebrated test of SUSY, but from the above comparison we see that it is only a necessary, but not a sufficient condition in proving supersymmetry. In addition, the measurement of superpartner couplings in order to test the SUSY relations is a very challenging task at a hadron collider. For one, the observed production rate in any given channel is only sensitive to the product of the cross-section times the branching fractions, and so any attempt to measure the couplings from a cross-section would have to make certain assumptions about the branching fractions. An additional complication arises from the fact that at hadron colliders all kinematically available states can be produced simultaneously, and the production of a particular species in an exclusive channel is rather difficult to isolate. The couplings could also in principle be measured from the branching fractions, but that also requires a measurement of the total width, which is impossible in our case, since the Breit-Wigner resonance cannot be reconstructed, due to the unknown momentum of the missing LSP (LKP).

We are therefore forced to concentrate on the first two identifying features as the only promising discriminating criteria. Let us begin with feature 1: the number of new particles. The KK particles at  $n = 1$  are analogous to superpartners in supersymmetry. However, the particles at the higher KK levels have no analogues in  $N = 1$  supersymmetric models.

---

<sup>2</sup> Strictly speaking, the number of KK modes is  $\Lambda R$ , see Section II A.



Discovering the  $n \geq 2$  levels of the KK tower would therefore indicate the presence of extra dimensions rather than SUSY. In this study we shall concentrate on the  $n = 2$  level and in Section III we investigate the discovery opportunities at the LHC and the Tevatron (for linear collider studies of  $n = 2$  KK gauge bosons, see [4, 6, 7, 13]). Notice that the masses of the KK modes are given roughly by  $m_n \sim n/R$ , where  $n$  is the KK level number, so that the particles at levels 3 and higher are rather heavy and their production is severely suppressed.

The second identifying feature – the spins of the new particles – also provides a tool for discrimination between SUSY and UED: the KK partners have identical spin quantum numbers as their SM counterparts, while the spins of the superpartners differ by 1/2 unit. However, spin determinations are known to be difficult at the LHC (or at hadron colliders in general), where the parton-level center of mass energy  $E_{CM}$  in each event is unknown. In addition, the momenta of the two dark matter candidates in the event are also unknown. This prevents the reconstruction of any rest frame angular decay distributions, or the directions of the two particles at the top of the decay chains. The variable  $E_{CM}$  also rules out the possibility of a threshold scan, which is one of the main tools for determining particle spins at lepton colliders. We are therefore forced to look for new methods for spin determinations, or at least for finding spin correlations<sup>3</sup>. Recently it has been suggested that a charge asymmetry in the lepton-jet invariant mass distributions from a particular cascade, can be used to discriminate SUSY from the case of pure phase space decays [9]. The possibility of discriminating SUSY and UED by this method will be the subject of Section IV (see also [10, 11, 12, 13] and [14]).

For the purposes of our study we have implemented the relevant features of the Minimal UED model in the **CompHEP** event generator [63]. The Minimal Supersymmetric Standard Model (MSSM) is already available in **CompHEP** since version 41.10. We incorporated all  $n = 1$  and  $n = 2$  KK modes as new particles, with the proper interactions, widths, and

---

<sup>3</sup> Notice that in simple processes with two-body decays like slepton production  $e^+e^- \rightarrow \tilde{\mu}^+\tilde{\mu}^- \rightarrow \mu^+\mu^-\tilde{\chi}_1^0\tilde{\chi}_1^0$  the flat energy distribution of the observable final state particles (muons in this case) is often regarded as a smoking gun for the scalar nature of the intermediate particles (the smuons). Indeed, the smuons are spin zero particles and decay isotropically in their rest frame, which results in a flat distribution in the lab frame. However, the flat distribution is a necessary but not sufficient condition for a scalar particle, and UED provides a counterexample with the analogous process of KK muon production [4], where a flat distribution also appears, but as a result of equal contributions from left-handed and right-handed KK fermions.

one-loop corrected masses [26]. Similar to the SM case, the neutral gauge bosons at level 1,  $Z_1$  and  $\gamma_1$ , are mixtures of the KK modes of the hypercharge gauge boson and the neutral  $SU(2)_W$  gauge boson. However, as shown in [26], the radiatively corrected Weinberg angle at level 1 and higher is very small. For example,  $\gamma_1$ , which is the LKP in the minimal UED model, is mostly the KK mode of the hypercharge gauge boson. For simplicity, in the code we neglected neutral gauge boson mixing for  $n \geq 1$ .

### III. COLLIDER SEARCH FOR LEVEL 2 KK PARTICLES

In this section we shall consider the prospects for discovery of level 2 Kaluza-Klein particles in UED. Our notation and conventions follow those of Ref. [2]. For example,  $SU(2)_W$ -doublet ( $SU(2)_W$ -singlet) KK fermions are denoted by capital (lowercase) letters. The KK level  $n$  is denoted by a subscript.

#### A. Phenomenology of Level 2 Fermions

We begin our discussion with the  $n = 2$  KK fermions. Since the KK mass spectrum is pretty degenerate, the production cross-sections at the LHC are mostly determined by the strength of the KK particle interactions with the proton constituents. As KK quarks carry color, we expect their production rates to be much higher than those of KK leptons. We shall therefore concentrate on the case of KK quarks only.

In principle, there are two mechanisms for producing  $n = 2$  KK quarks at the LHC: through KK-number conserving interactions, or through KK-number violating (but KK-parity conserving) interactions. The KK number conserving QCD interactions allow production of KK quarks either in pairs or singly (in association with the  $n = 2$  KK mode of a gauge boson). The corresponding production cross-sections are shown in Fig. 2 (the cross-sections for producing  $n = 1$  KK quarks have been calculated in [14, 64, 65]). In Fig. 2a we show the cross-sections (in pb) for  $n = 2$  KK-quark pair production, while in Fig. 2b we show the results for  $n = 2$  KK-quark/KK-gluon associated production and for  $n = 2$  KK-gluon pair production. We plot the results versus  $R^{-1}$ , and one should keep in mind that the masses of the  $n = 2$  particles are roughly  $2/R$ . In calculating the cross-sections of Fig. 2 we consider 5 partonic quark flavors in the proton along with the gluon. We sum over

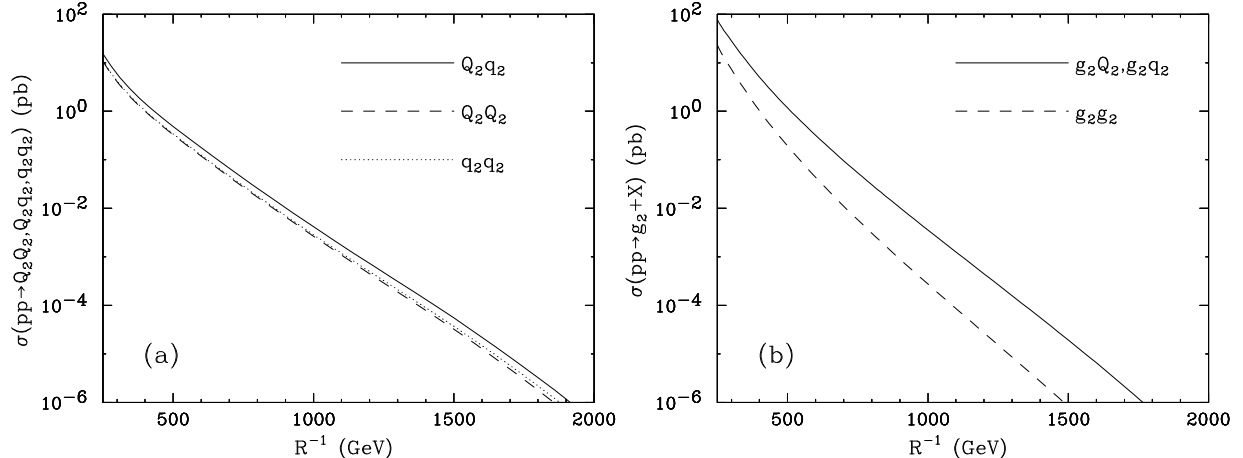


FIG. 2: Strong production of  $n = 2$  KK particles at the LHC: (a) KK-quark pair production; (b) KK-quark/KK-gluon associated production and KK-gluon pair production. The cross-sections have been summed over all quark flavors and also include charge-conjugated contributions such as  $Q_2\bar{q}_2$ ,  $\bar{Q}_2q_2$ ,  $g_2\bar{Q}_2$ , etc.

the final state quark flavors and include charge-conjugated contributions. We used CTEQ5L parton distributions [66] and choose the scale of the strong coupling constant  $\alpha_s$  to be equal to the parton level center of mass energy. All calculations are done with CompHEP [63] with our implementation of the Minimal UED model.

Several comments are in order. First, Fig. 2 displays a severe kinematic suppression of the cross-sections at large KK masses. This is familiar from the case of SUSY, where the ultimate LHC reach for colored superpartners extends only to about 3 TeV. Notice the different mass dependence of the cross-sections for the three types of final states with  $n = 2$  particles: quark-quark, quark-gluon, and gluon-gluon. This can be easily understood in terms of the structure functions of the quarks and gluon inside the proton. We also observe minor differences in the cross-sections for pair production of KK quarks with different  $SU(2)_W$  quantum numbers. This is partially due to the different masses for  $SU(2)_W$ -doublet and  $SU(2)_W$ -singlet quarks (see Fig. 1), and the remaining difference is due to the contributions from diagrams with electroweak gauge bosons. Notice that since the cross-sections in Fig. 2a are summed over charge conjugated final states, the mixed case of  $Q_2q_2$  contains twice as many quark-antiquark contributions (compare  $Q_2\bar{q}_2 + \bar{Q}_2q_2$  to  $q_2\bar{q}_2$  or  $Q_2\bar{Q}_2$  alone).

If we compare the cross-sections for  $n = 2$  KK quark production to the cross-sections for producing squarks of similar masses in SUSY, we realize that the production rates are

higher in UED. This is due to several reasons. Consider, for example,  $s$ -channel processes. Well above threshold, the UED cross-sections are larger by a factor of 4 [4]. One factor of 2 is due to the fact that in UED the particle content at  $n \geq 1$  is duplicated – for example, there are both left-handed and right-handed  $SU(2)_W$ -doublet KK fermions, while in SUSY there are only “left-handed”  $SU(2)_W$ -doublet squarks. Another factor of 2 comes from the different angular distribution for fermions,  $1 + \cos^2 \theta$ , versus scalars,  $1 - \cos^2 \theta$ . When integrated over all angles, this accounts for the second factor of 2 difference. Furthermore, at the LHC new heavy particles are produced close to threshold, due to the steeply falling parton luminosities. In SUSY, the new particles (squarks) are scalars, and the threshold suppression of the cross-sections is  $\sim \beta^3$ , while in UED the KK-quarks are fermions, and the threshold suppression of the cross-section is only  $\beta$ . This distinct threshold behavior of the production cross-sections further enhances the difference between SUSY and UED. For example, we find that for  $R^{-1} = 500$  GeV the pair production cross-section for charm KK-quarks is about 6 times larger than the cross-section for charm squarks. For processes involving first generation KK-quarks, where  $t$ -channel diagrams contribute significantly, the effect can be even bigger. For example, up KK-quark production and up squark production differ by about factor of 8.

In Fig. 2 we have only considered production due to KK number conserving bulk interactions. The main advantage of those processes is that the corresponding couplings are unsuppressed. However, the disadvantage is that we need to produce *two* heavy particles, each of mass  $\sim 2/R$ , which leads to a kinematic suppression. In order to overcome this problem, one could in principle consider the single production of  $n = 2$  KK quarks through KK number violating, but KK parity conserving interactions, for example

$$\bar{Q}_2 \gamma^\mu T^a P_L Q_0 A_{0\mu}^a, \quad (1)$$

where  $A_\mu^a$  is a SM gauge field and  $T^a$  is the corresponding group generator. However, (1) is forbidden by gauge invariance, and the lowest order coupling of an  $n = 2$  KK quark to two SM particles has the form [26]

$$\bar{Q}_2 \sigma^{\mu\nu} T^a P_L Q_0 F_{0\mu\nu}^a. \quad (2)$$

Such operators may in principle be present, as they may be generated at the scale  $\Lambda$  by the unknown physics at higher scales. However, being higher dimensional, we expect them to be suppressed at least by  $1/\Lambda$ , hence in our subsequent analysis we shall neglect them.

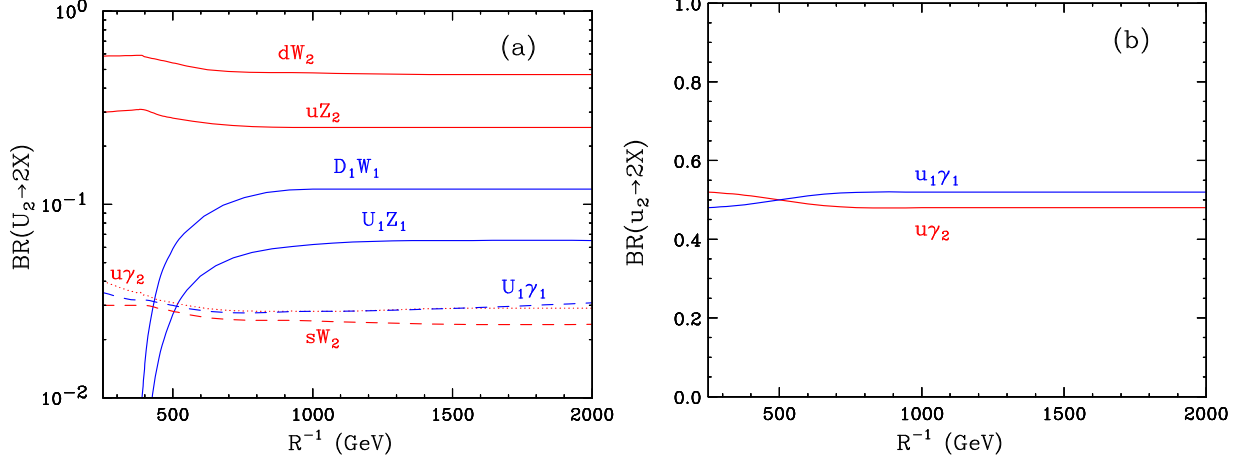


FIG. 3: Branching fractions of the level 2 “up” quarks versus  $R^{-1}$ ; for (a) the  $SU(2)_W$ -doublet quark  $U_2$  and (b) the  $SU(2)_W$ -singlet quark  $u_2$ .

Having determined the production rates of level 2 KK quarks, we now turn to the discussion of their experimental signatures. To this end we need to determine the possible decay modes of  $Q_2$  and  $q_2$ . At each level  $n$ , the KK quarks are among the heaviest states in the KK spectrum and can decay promptly to lighter KK modes (this is true for the top KK modes [67, 68] as well). As can be seen from Fig. 1, the KK gluon is always heavier than the KK quarks, so the two body decays of KK quarks to KK gluons are closed. Instead,  $n = 2$  KK quarks will decay to the KK modes of the electroweak gauge bosons which are lighter. The branching fractions for  $n = 2$  “up”-type KK quarks are shown in Fig. 3. Fig. 3a (Fig. 3b) is for the case of the  $SU(2)_W$ -doublet quark  $U_2$  (the  $SU(2)_W$ -singlet quark  $u_2$ ). The results for the “down”-type KK quarks are similar. We observe in Fig. 3 that the branching fractions are almost independent of  $R^{-1}$ , unless one is close to threshold. This feature will persist for all branching ratios of KK particles which will be shown later.

Once we ignore the KK number violating coupling (2), only decays which conserve the total KK number  $n$  are allowed. The case of the  $SU(2)_W$ -singlet quarks such as  $u_2$  is simpler, since they only couple to the hypercharge gauge bosons. Recall that at  $n \geq 1$  the hypercharge component is almost entirely contained in the  $\gamma$  KK mode [26]. We therefore expect a singlet KK quark  $q_2$  to decay to either  $q_1\gamma_1$  or  $q_0\gamma_2$ , as seen in Fig. 3b. The case of an  $SU(2)_W$ -doublet quark  $Q_2$  is much more complicated, since  $Q_2$  couples to the (KK modes of the) weak gauge bosons as well, and many more two-body final states are possible. Since the weak coupling is larger than the hypercharge coupling, the decays to  $W$  and  $Z$  KK modes

dominate, with  $BR(Q_2 \rightarrow Q'_0 W_2)/BR(Q_2 \rightarrow Q_0 Z_2) = 2$  and  $BR(Q_2 \rightarrow Q'_1 W_1)/BR(Q_2 \rightarrow Q_1 Z_1) = 2$ , as evidenced in Fig. 3a. The branching fractions to the  $\gamma$  KK modes are only on the order of a few percent. The threshold behavior seen in Fig. 3a near  $R^{-1} = 400$  GeV is due to the finite masses for the SM  $W$  and  $Z$  bosons, which enter the tree-level masses of  $W_1^\pm$  and  $Z_1$ . Since the mass splitting of the KK modes is due to the radiative corrections, which are proportional to  $R^{-1}$ , the channels with  $W_1^\pm$  and  $Z_1$  open up only for sufficiently large  $R^{-1}$ .

We are now in a position to discuss the experimental signatures of  $n = 2$  KK quarks. The decays to level 2 gauge bosons will simply contribute to the inclusive production of  $\gamma_2$ ,  $Z_2$  and  $W_2^\pm$ , which will be discussed at length later in Section III B. On the other hand, the decays to two  $n = 1$  KK modes will contribute to the inclusive production of  $n = 1$  KK particles which was discussed in [2]. Naturally, the direct pair production of the lighter  $n = 1$  KK modes has a much larger cross-section. Therefore, the indirect production of  $n = 1$  KK modes from the decays of  $n = 2$  particles can be easily swamped by the direct  $n = 1$  signals and the SM backgrounds. For example, the experimental signature for an  $n = 2$  KK quark decaying as  $Q_2 \rightarrow Q_1 \gamma_1$  ( $q_2 \rightarrow q_1 \gamma_1$ ) is indistinguishable from a single  $Q_1$  ( $q_1$ ). This is because  $\gamma_1$  does not interact within the detector, and there are at least two additional  $\gamma_1$  particles in each event, so that we cannot determine how many  $\gamma_1$  particles caused the measured amount of missing energy. The decays to  $W_1$  and  $Z_1$  may, however, lead to final states with up to four  $n = 1$  particles, each with a leptonic decay mode. The resulting multilepton signatures  $N\ell + \cancel{E}_T$  with  $N \geq 5$  are therefore very clean and potentially observable. Distinguishing those events from direct  $n = 1$  pair production would be an important step in establishing the presence of the  $n = 2$  level of the quark KK tower. Unfortunately, the  $n = 2$  sample is statistically very limited and this analysis appears very challenging. We postpone it for future work [69].

Much of the previous discussion applies directly to the level 2 KK leptons. Assuming the absence of the KK number violating coupling analogous to (2), the branching fractions of the  $n = 2$  KK electrons are shown in Fig. 4. At each KK level, the KK modes of the weak gauge bosons are heavier than the KK leptons, therefore the only allowed decays are to  $\gamma_2$  and  $\gamma_1$ . Just like KK quarks, KK leptons can be produced directly, through KK number conserving couplings, or indirectly, in  $W_2^\pm$  and  $Z_2$  decays. In either case, the resulting cross-sections are too small to be of interest at the LHC.

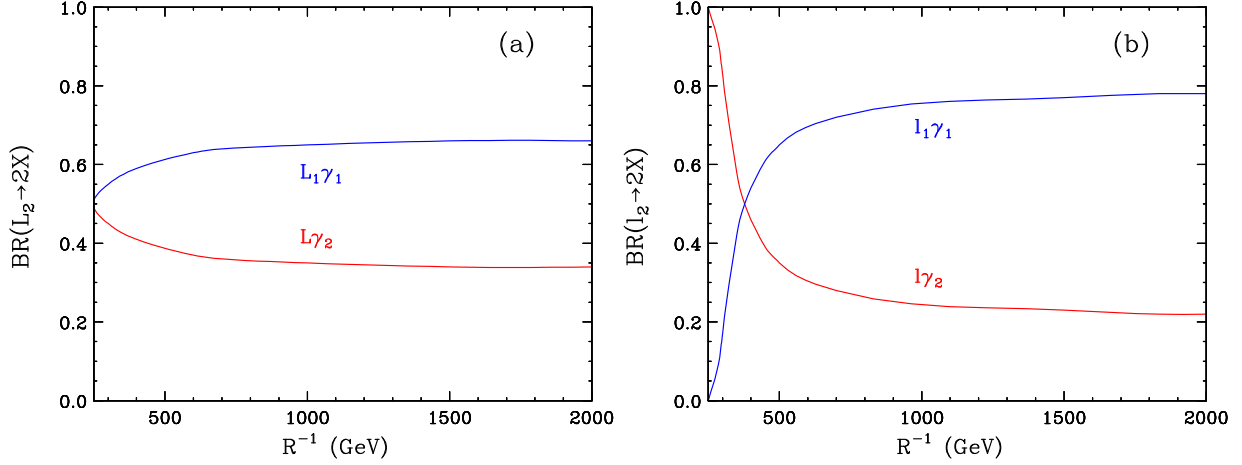


FIG. 4: The same as Fig. 3 but for the level 2 KK electrons: (a) the  $SU(2)_W$ -doublet  $E_2$  and (b) the  $SU(2)_W$ -singlet  $e_2$ .

## B. Level 2 Gauge Bosons

We now discuss the collider phenomenology of the  $n = 2$  gauge bosons  $V_2$ . As we shall see, the KK gauge bosons offer the best prospects for detecting the  $n = 2$  structure, since they have direct (but not tree level) couplings to SM particles, and can be discovered as resonances, e.g. in the dijet or dilepton channels. This is in contrast to the case of  $n = 2$  KK fermions, which, under the assumptions of Sec. III A, do not have fully visible decay modes. Bump hunting will also help discriminate between  $n = 2$  and  $n = 1$  KK particles, since the latter are KK-parity odd, and necessarily decay to the invisible  $\gamma_1$ .

There are four  $n = 2$  KK gauge bosons: the KK “photon”  $\gamma_2$ , the KK “ $Z$ -boson”  $Z_2$ , the KK “ $W$ -boson”  $W_2^\pm$ , and the KK gluon  $g_2$ . Recall that the Weinberg angle at  $n = 2$  is very small, so that  $\gamma_2$  is mostly the KK mode of the hypercharge gauge boson and  $Z_2$  is mostly the KK mode of the neutral  $W$ -boson of the SM. An important consequence of the extra dimensional nature of the model is that all four of the  $n = 2$  KK gauge bosons are relatively degenerate, as shown in Fig. 5a. The masses are all roughly equal to  $2/R$ . The mass splitting between the KK gauge bosons is almost entirely due to radiative corrections, which in the Minimal UED model yield the mass hierarchy  $m_{g_2} > m_{W_2} \sim m_{Z_2} > m_{\gamma_2}$ . The KK gluon receives the largest corrections and is the heaviest particle in the KK spectrum at each level  $n$ . The  $W_2^\pm$  and  $Z_2$  particles are degenerate to a very high degree, due to  $SU(2)_W$  symmetry.

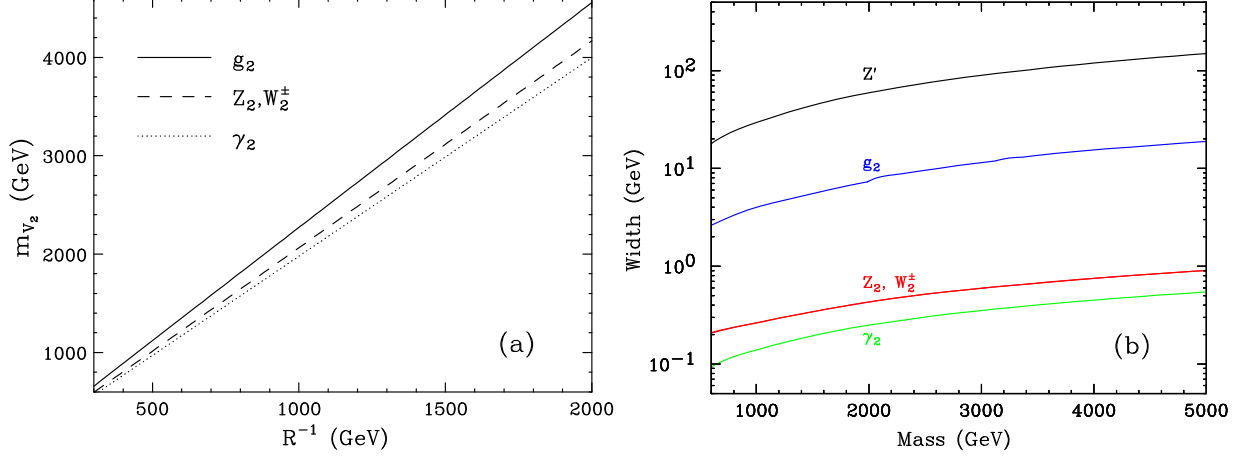


FIG. 5: (a) Masses of the four  $n = 2$  KK gauge bosons as a function of  $R^{-1}$ . (b) Total widths of the  $n = 2$  KK gauge bosons as a function of the corresponding mass. We also show the width of a generic  $Z'$  whose couplings to the SM particles are the same as those of the  $Z$ -boson.

The KK number conserving interactions allow an  $n = 2$  KK gauge boson  $V_2$  to decay to two  $n = 1$  particles, or to one  $n = 2$  KK particle and one  $n = 0$  (i.e., Standard Model) particle, provided that the decays are allowed by phase space. For example, the partial widths to fermion final states are given by

$$\begin{aligned}
\Gamma(V_2 \rightarrow f_2 \bar{f}_0) &= \frac{c^2 g^2}{48\pi m_{V_2}^3} \left( m_{V_2}^2 - m_{f_2}^2 - m_{f_0}^2 + \frac{m_{V_2}^4 - (m_{f_2}^2 - m_{f_0}^2)^2}{m_{V_2}^2} \right) \\
&\quad \times \sqrt{(m_{V_2}^2 - (m_{f_2} - m_{f_0})^2) (m_{V_2}^2 - (m_{f_2} + m_{f_0})^2)} \\
&\approx \frac{c^2 g^2}{48\pi m_{V_2}^3} (m_{V_2}^2 - m_{f_2}^2)^2 \left( 1 + \frac{m_{V_2}^2 + m_{f_2}^2}{m_{V_2}^2} \right) \\
&\approx \frac{c^2 g^2 m_{V_2}}{4\pi} \left( \frac{\hat{\delta} m_{V_2}}{m_2} - \frac{\hat{\delta} m_{f_2}}{m_2} \right)^2,
\end{aligned} \tag{3}$$

$$\begin{aligned}
\Gamma(V_2 \rightarrow f_1 \bar{f}_1) &= \frac{c^2 g^2}{24\pi m_{V_2}^2} (m_{V_2}^2 - 4m_{f_1}^2)^{\frac{3}{2}} \\
&\approx \frac{c^2 g^2 m_{V_2}}{6\sqrt{2}\pi} \left( \frac{\hat{\delta} m_{V_2}}{m_2} - \frac{\hat{\delta} m_{f_1}}{m_1} \right)^{\frac{3}{2}} \left( \frac{m_2}{m_{V_2}} \right)^3 \\
&\approx \frac{c^2 g^2 m_{V_2}}{6\sqrt{2}\pi} \left( \frac{\hat{\delta} m_{V_2}}{m_2} - \frac{\hat{\delta} m_{f_1}}{m_1} \right)^{\frac{3}{2}},
\end{aligned} \tag{4}$$

where  $c \approx Y N_c^f / 2$  for  $V_2 \approx \gamma_2$ ,  $c \approx N_c^f / 2$  for  $V_2 \approx Z_2$ ,  $c = V_{CKM} N_c^f / \sqrt{2}$  for  $V_2 = W_2^\pm$  and  $c = 1/\sqrt{2}$  for  $V_2 = g_2$ , with  $Y$  being the fermion hypercharge in the normalization



$Q = T_3 + Y/2$ ,  $V_{CKM}$  is the CKM mixing matrix, and  $N_c^f = 3$  for  $f = q$  and  $N_c^f = 1$  for  $f = \ell$ . Here  $\hat{\delta}m$  stands for the total radiative correction to a KK mass  $m$ , including both bulk and boundary contributions [26],  $m_2 \equiv 2/R$ , and  $g$  is the corresponding gauge coupling. The first lines in (3) and (4) give the exact result, while the last lines are the approximate formulas derived in [2] as leading order expansions in  $\hat{\delta}m/m$ . The second line in (3) is an approximation neglecting the SM fermion mass  $m_{f_0}$ . The second line in (4) is an alternative approximation which incorporates subleading but numerically important terms. In our code we have programmed the exact expressions and quote the approximations here only for completeness.

Note that the KK number conserving decays of the  $n = 2$  KK gauge bosons are suppressed by phase space. This is evident from the approximate expressions in eqs. (3) and (4). The partial widths are proportional to the one-loop corrections, which open up the available phase space and allow the corresponding decay mode to take place. However, not all of the fermionic final states are available, for example,  $Z_2$  and  $W_2^\pm$  have no hadronic decay modes to level 1 or 2, while  $\gamma_2$  has *no* KK number conserving decay modes at all.

The  $n = 2$  KK gauge bosons also have KK number violating couplings which can be generated either radiatively from bulk interactions, or directly at the scale  $\Lambda$  [26]. For example, the operator

$$\bar{f}_0 \gamma^\mu T^a P_L f_0 A_{2\mu}^a \quad (5)$$

couples  $V_2$  directly to SM fermions  $f_0$ , and leads to the the following  $V_2$  partial width

$$\begin{aligned} \Gamma(V_2 \rightarrow f_0 \bar{f}_0) &= \frac{c^2 g^2 m_{V_2}}{12\pi} \left( \frac{\bar{\delta}m_{V_2}}{m_2} - \frac{\bar{\delta}m_{f_2}}{m_2} \right)^2 \left( 1 - \frac{m_{f_0}^2}{m_{V_2}^2} \right) \sqrt{\left( 1 - 4 \frac{m_{f_0}^2}{m_{V_2}^2} \right)} \\ &\approx \frac{c^2 g^2 m_{V_2}}{12\pi} \left( \frac{\bar{\delta}m_{V_2}}{m_2} - \frac{\bar{\delta}m_{f_2}}{m_2} \right)^2, \end{aligned} \quad (6)$$

where  $\bar{\delta}m$  stands for a mass correction due to boundary terms only [26]. In the second line we have neglected the SM fermion mass  $m_{f_0}$ , recovering the result from [2].

As we see from (6), the KK number violating decay is also suppressed, this time by a loop factor, and is proportional to the size of the radiative corrections to the corresponding KK masses. In spite of this suppression, the  $V_2 \rightarrow f_0 \bar{f}_0$  decays is most promising for experimental discovery. As long as the final state fermions can be reconstructed, the  $V_2$  particle can be looked for as a bump in the invariant mass distribution of its decay products. In this sense, the search is very similar to  $Z'$  searches, with one major difference. Since *all* partial widths

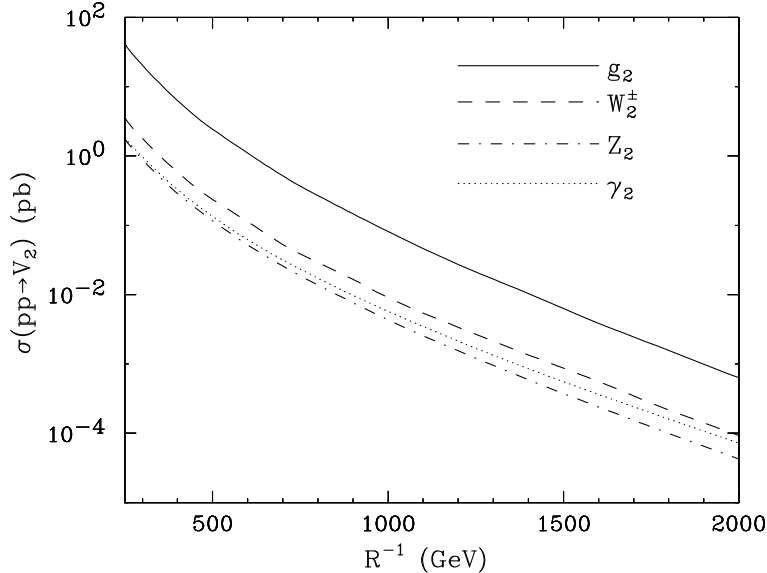


FIG. 6: Cross-sections for single production of level 2 KK gauge bosons through the KK number violating couplings (5).

(3-6) are suppressed, the *total* width of  $V_2$  is much smaller than the width of a typical  $Z'$ . This is illustrated in Fig. 5b, where we plot the widths of the KK particles  $\gamma_2$ ,  $W_2^\pm$ ,  $Z_2$  and  $g_2$  in UED, as a function of the corresponding particle mass, and contrast to the width of a  $Z'$  with SM-like couplings. We see that the widths of the KK gauge bosons are extremely small. This has important ramifications for the experimental search, since the width of the resonance will then be determined by the experimental resolution, rather than the intrinsic particle width. In this sense the width must be included in the set of basic parameters of a  $Z'$  search [70].

Before we elaborate on the experimental signatures of the  $n = 2$  KK gauge bosons, let us briefly discuss their production. There are three basic mechanisms:

**1. Single production through the KK number violating operator (5).** The corresponding cross-sections are shown in Fig. 6 as a function of  $R^{-1}$ . One might expect that these processes will be important, especially at large masses, since we need to make only a single heavy  $n = 2$  particle, alleviating the kinematic suppression. If we compare the mass dependence of the Drell-Yan cross-sections in Fig. 6 to the mass dependence of the  $n = 2$  pair production cross-sections from Fig. 2, indeed we see that the former drop less steeply with  $R^{-1}$  and become dominant at large  $R^{-1}$ . On the other hand, the Drell-Yan processes of Fig. 6 are mediated by a KK number violating operator (5) and the coupling

of a  $V_2$  to SM particles is radiatively suppressed. This is another crucial difference with the case of a generic  $Z'$ , whose couplings typically have the size of a normal gauge coupling and are unsuppressed [70].

Notice the roughly similar size of the four cross-sections shown in Fig. 6. This is somewhat surprising, since the cross-sections scale as the corresponding gauge coupling squared, and one would have expected a wider spread in the values of the four cross-sections. This is due to a couple of things. First, for a given  $R^{-1}$ , the masses of the four  $n = 2$  KK gauge bosons are different, with  $m_{g_2} > m_{W_2} \sim m_{Z_2} > m_{\gamma_2}$ . Therefore, for a given  $R^{-1}$ , the heavier particles suffer a suppression. This explains to an extent why the cross-section for  $\gamma_2$  is not the smallest of the four, and why the cross-section for  $g_2$  is not as large as one would expect. There is, however, a second effect, which goes in the same direction. The coupling (5) is also proportional to the mass corrections of the corresponding particles:

$$\frac{\bar{\delta}m_{V_2}}{m_{V_2}} - \frac{\bar{\delta}m_{f_2}}{m_{f_2}}. \quad (7)$$

Since the QCD corrections are the largest, for  $V_2 = \{\gamma_2, Z_2, W_2^\pm\}$ , the second term dominates. However, for  $V_2 = g_2$ , the first term is actually larger, and there is a cancellation, which further reduces the direct KK gluon couplings to quarks.

**2. Indirect production.** The electroweak KK modes  $\gamma_2$ ,  $Z_2$  and  $W_2^\pm$  can be produced in the decays of heavier  $n = 2$  particles such as the KK quarks and/or KK gluon. This is well known from the case of SUSY, where the dominant production of electroweak superpartners is often indirect – from squark and gluino decay chains. The indirect production rates of  $\gamma_2$ ,  $Z_2$  and  $W_2^\pm$  due to QCD processes can be readily estimated from Figs. 2 and 3. Notice that  $BR(Q_2 \rightarrow W_2^\pm)$ ,  $BR(Q_2 \rightarrow Z_2)$  and  $BR(q_2 \rightarrow \gamma_2)$  are among the largest branching fractions of the  $n = 2$  KK quarks, and we expect indirect production from QCD to be a significant source of electroweak  $n = 2$  KK modes.

**3. Direct pair production.** The  $n = 2$  KK modes can also be produced directly in pairs, through KK number conserving interactions. These processes, however, are kinematically suppressed, since we have to make *two* heavy particles in the final state. One would therefore expect that they will be the least relevant source of  $n = 2$  KK gauge bosons. The only exception is KK gluon pair production which is important and is shown in Fig. 2b. We see that it is comparable in size to KK quark pair production and  $q_2 g_2 / Q_2 g_2$  associated production. We have also calculated the pair production cross-sections for the electroweak

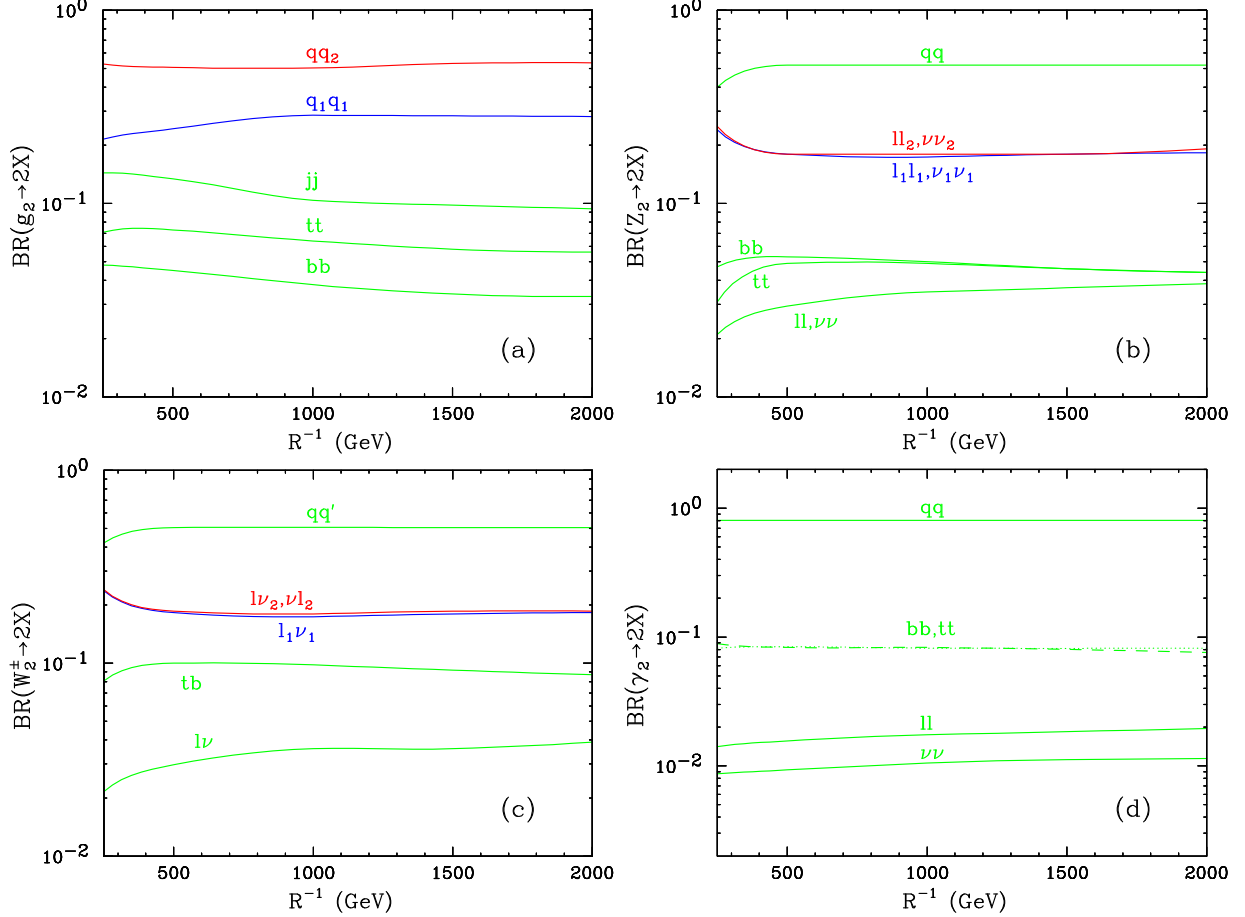


FIG. 7: Branching fractions of the  $n = 2$  KK gauge bosons versus  $R^{-1}$ : (a)  $g_2$ , (b)  $Z_2$ , (c)  $W_2^\pm$ , and (d)  $\gamma_2$ .

$n = 2$  KK gauge bosons and confirmed that they are very small, hence we shall neglect them in our analysis below.

In conclusion of this section, we discuss the experimental signatures of  $n = 2$  KK gauge bosons. To this end, we need to consider their possible decay modes. Having previously discussed the different partial widths, it is straightforward to compute the  $V_2$  branching fractions. Those are shown in Fig. 7(a-d). Again we observe that the branching fractions are very weakly sensitive to  $R^{-1}$ , just as the case of Figs. 3 and 4. This can be understood as follows. The partial widths (3) and (4) for the KK number conserving decays are proportional to the available phase space, while the partial width (6) for the KK number violating decay is proportional to the mass corrections (see eq. (7)). Both the phase space and the mass corrections are proportional to  $R^{-1}$ , which then cancels out in the branching fraction.

Similarly to the case of  $n = 2$  KK quarks discussed in Sec. III A, KK number conserving

decays are not very distinctive, since they simply contribute to the inclusive  $n = 1$  sample which is dominated by direct  $n = 1$  production. The decays of  $n = 1$  particles will then give relatively soft objects, and most of the energy will be lost in the LKP mass. In short,  $n = 2$  signatures based on purely KK number conserving decays are not very promising experimentally — one has to pay a big price in the cross-section in order to produce the heavy  $n = 2$  particles, but does not get the benefit of the large mass, since most of the energy is carried away by the invisible LKP. We therefore concentrate on the KK number violating channels, in which the  $V_2$  decays are fully visible.

Fig. 7a shows the branching fractions of the KK gluon  $g_2$ . Since it is the heaviest particle at level 2, all of its decay modes are open, and have comparable branching fractions. The KK number conserving decays dominate, since the KK number violating coupling is slightly suppressed due to the cancellation in (7). In principle,  $g_2$  can be looked for as a resonance in the dijet [71] or  $t\bar{t}$  invariant mass spectrum, but one would expect large backgrounds from QCD and Drell-Yan. Notice that there is no indirect production of  $g_2$ , and its single production cross-section is not that much different from the cross-sections for  $\gamma_2$ ,  $Z_2$  and  $W_2^\pm$  (see Fig. 6). Therefore, the inclusive  $g_2$  production is comparable to the inclusive  $\gamma_2$  and  $Z_2$  production, and then we anticipate that the searches for the  $n = 2$  electroweak gauge bosons in leptonic channels will be more promising.

Figs. 7b and 7c give the branching fractions of  $Z_2$  and  $W_2^\pm$ , correspondingly. We see that the decays to KK quarks have been closed due to the large QCD radiative corrections to the KK quark masses. Among the possible KK number conserving decays of  $Z_2$  and  $W_2^\pm$ , only the leptonic modes survive, and they will be contributing to the leptonic discovery signals of UED [2]. Recall that the KK number conserving decays are phase space suppressed, while the KK number violating decays are loop suppressed, and proportional to the mass corrections as in (7). The precise calculation shows that the dominant decay modes are  $Z_2 \rightarrow q\bar{q}$  and  $W_2^\pm \rightarrow q\bar{q}'$ . This can be understood in terms of the large  $\bar{\delta}m_{q_2}$  correction appearing in (7). The resulting branching ratios are more than 50% and in principle allow for a  $Z_2/W_2^\pm$  search in the dijet channel, just like the case of  $g_2$ . However, we shall concentrate on the leptonic decay modes, which have much smaller branching fractions, but are much cleaner experimentally.

Finally, Fig. 7d shows the branching fractions of  $\gamma_2$ . This time all KK number conserving decays are closed, and  $\gamma_2$  is forced to decay through the KK number violating interaction (5).

Again, the jetty modes dominate, and the leptonic modes (summed over lepton flavors) have rather small branching fractions, on the order of 2%, which could be a potential problem for the search. In the following section we shall concentrate on the  $Z_2 \rightarrow \ell^+\ell^-$  and  $\gamma_2 \rightarrow \ell^+\ell^-$  signatures and analyze their discovery prospects in a  $Z'$ -like search [72, 73].

### C. Analysis of the LHC reach for $Z_2$ and $\gamma_2$

We are now in a position to discuss the discovery reach of the  $n = 2$  KK gauge bosons at the LHC and the Tevatron. We will consider the inclusive production of  $Z_2$  and  $\gamma_2$  and look for a dilepton resonance in both the  $e^+e^-$  and  $\mu^+\mu^-$  channels. An important parameter of the search is the width of the reconstructed resonance, which in turn determines the size of the invariant mass window selected by the cuts. Since the intrinsic width of the  $Z_2$  and  $\gamma_2$  resonances is so small (see Fig. 5b), the mass window is entirely determined by the mass resolution in the dimuon and dielectron channels. For electrons, the resolution in CMS is approximately constant, on the order of  $\Delta m_{ee}/m_{ee} \approx 1\%$  in the region of interest [74]. On the other hand, the dimuon mass resolution is energy dependent, and in preliminary studies based on a full simulation of the CMS detector has been parametrized as [75]

$$\frac{\Delta m_{\mu\mu}}{m_{\mu\mu}} = 0.0215 + 0.0128 \left( \frac{m_{\mu\mu}}{1 \text{ TeV}} \right) .$$

Therefore in our analysis we impose the following cuts

1. Lower cuts on the lepton transverse momenta  $p_T(\ell) > 20$  GeV.
2. Central rapidity cut on the leptons  $|\eta(\ell)| < 2.4$ .
3. Dilepton invariant mass cut for electrons  $m_{V_2} - 2\Delta m_{ee} < m_{ee} < m_{V_2} + 2\Delta m_{ee}$  and muons  $m_{V_2} - 2\Delta m_{\mu\mu} < m_{\mu\mu} < m_{V_2} + 2\Delta m_{\mu\mu}$ .

With these cuts the signal efficiency varies from 65% at  $R^{-1} = 250$  GeV to 91% at  $R^{-1} = 1$  TeV. The main SM background to our signal is Drell-Yan, which we have calculated with the PYTHIA event generator [76].

With the cuts listed above, we compute the discovery reach of the LHC and the Tevatron for the  $\gamma_2$  and  $Z_2$  resonances. Our results are shown in Fig. 8. We plot the total integrated luminosity  $L$  (in  $\text{fb}^{-1}$ ) required for a  $5\sigma$  excess of signal over background in the dielectron

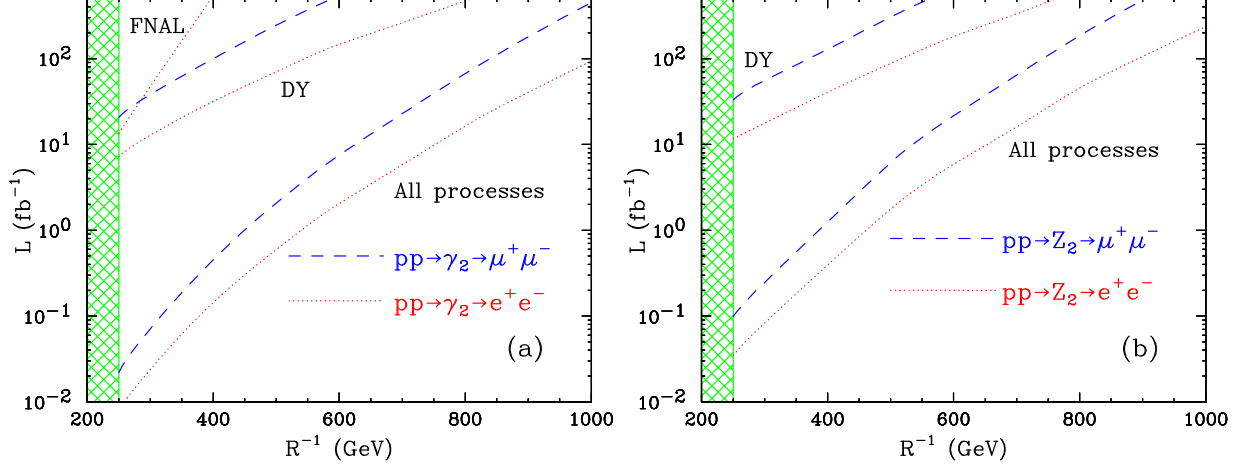


FIG. 8:  $5\sigma$  discovery reach for (a)  $\gamma_2$  and (b)  $Z_2$ . We plot the total integrated luminosity  $L$  (in  $\text{fb}^{-1}$ ) required for a  $5\sigma$  excess of signal over background in the dielectron (red, dotted) or dimuon (blue, dashed) channel, as a function of  $R^{-1}$ . In each plot, the upper set of lines labelled “DY” makes use of the single  $V_2$  production of Fig. 6 only, while the lower set of lines (labelled “All processes”) includes indirect  $\gamma_2$  and  $Z_2$  production from  $n = 2$  KK quark decays. The red dotted line marked “FNAL” in the upper left corner of (a) reflects the expectations for a  $\gamma_2 \rightarrow e^+e^-$  discovery at the Tevatron in Run II. The shaded area below  $R^{-1} = 250$  GeV indicates the region disfavored by precision electroweak data [31].

(red, dotted) or dimuon (blue, dashed) channel, as a function of  $R^{-1}$ . In each panel in Fig. 8, the upper set of lines labelled “DY” only utilizes the single  $V_2$  production cross-sections from Fig. 6. The lower set of lines (labelled “All processes”) includes in addition indirect  $\gamma_2$  and  $Z_2$  production from the decays of  $n = 2$  KK quarks to  $\gamma_2$  and  $Z_2$  (we ignore secondary  $\gamma_2$  production from  $Q_2 \rightarrow Z_2 \rightarrow \ell_2 \rightarrow \gamma_2$ ). The shaded area below  $R^{-1} = 250$  GeV indicates the region disfavored by precision electroweak data [31]. Using the same cuts also for the case of the Tevatron, we find the Tevatron reach in  $\gamma_2 \rightarrow e^+e^-$  shown in Fig. 8a and labelled “FNAL”. For the Tevatron we use electron energy resolution  $\Delta E/E = 0.01 \oplus 0.16/\sqrt{E}$  [77]. The Tevatron reach in dimuons is worse due to the poorer resolution, while the reach for  $Z_2$  is also worse since  $m_{Z_2} > m_{\gamma_2}$  for a fixed  $R^{-1}$ .

Fig. 8 reveals that there are good prospects for discovering level 2 gauge boson resonances at the LHC. Already within one year of running at low luminosity ( $L = 10 \text{ fb}^{-1}$ ), the LHC will have sufficient statistics in order to probe the region up to  $R^{-1} \sim 750$  GeV. Notice that

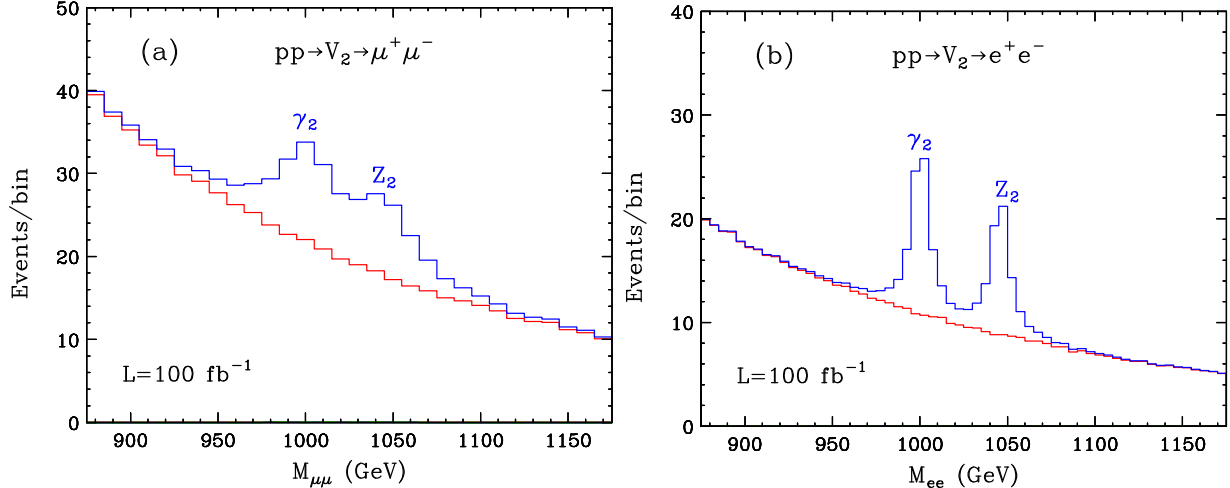


FIG. 9: The  $\gamma_2 - Z_2$  diresonance structure in UED with  $R^{-1} = 500$  GeV, for (a) the dimuon and (b) the dielectron channel at the LHC with  $L = 100 \text{ fb}^{-1}$ . The SM background is shown with the (red) continuous underlying histogram.

in the Minimal UED model, the “good dark matter” region, where the LKP relic density accounts for all of the dark matter component of the Universe, is at  $R^{-1} \sim 500 - 600$  GeV [39, 43, 44]. This region is well within the discovery reach of the LHC for both  $n = 1$  KK modes [2] and  $n = 2$  KK gauge bosons (Fig. 8). If the LKP accounts for only *a fraction* of the dark matter, the preferred range of  $R^{-1}$  is even lower and the discovery at the LHC is easier.

From Fig. 8 we also see that the ultimate reach of the LHC for both  $\gamma_2$  and  $Z_2$ , after several years of running at high luminosity ( $L \sim 300 \text{ fb}^{-1}$ ), extends up to just beyond  $R^{-1} = 1$  TeV. One should keep in mind that the actual KK masses are at least twice as large:  $m_{V_2} \sim m_2 = 2/R$ , so that the KK resonances can be discovered for masses up to 2 TeV.

While the  $n = 2$  KK gauge bosons are a salient feature of the UED scenario, any such resonance by itself is not a sufficient discriminator, since it resembles an ordinary  $Z'$  gauge boson. If UED is discovered, one could then still make the argument that it is in fact some sort of non-minimal supersymmetric model with an additional gauge structure containing neutral gauge bosons. An important corroborating evidence in favor of UED would be the simultaneous discovery of several, rather degenerate, KK gauge boson resonances. While SUSY also can accommodate multiple  $Z'$  gauge bosons, there would be no good motivation



behind their mass degeneracy. A crucial question therefore arises: can we separately discover the  $n = 2$  KK gauge bosons as individual resonances? For this purpose, one would need to see a double peak structure in the invariant mass distributions. Clearly, this is rather challenging in the dijet channel, due to the relatively poor jet energy resolution. We shall therefore consider only the dilepton channels, and investigate how well we can separate  $\gamma_2$  from  $Z_2$ .

Our results are shown in Fig. 9, where we show the invariant mass distribution in UED with  $R^{-1} = 500$  GeV, for (a) the dimuon and (b) the dielectron channel at the LHC with  $L = 100 \text{ fb}^{-1}$ . We see that the diresonance structure is easier to detect in the dielectron channel, due to the better mass resolution. In dimuons, with  $L = 100 \text{ fb}^{-1}$  the structure is also beginning to emerge. We should note that initially the two resonances will not be separately distinguishable, and each will in principle contribute to the discovery of a bump, although with a larger mass window. In our reach plots in Fig. 8 we have conservatively chosen not to combine the two signals from  $Z_2$  and  $\gamma_2$ , but show the reach for each one separately.

#### IV. SPIN DISCRIMINATIONS IN SUSY AND UED

As discussed in Section I, the second fundamental distinction between UED and supersymmetry is reflected in the properties of the individual particles: the KK partners have identical spin quantum numbers as their SM counterparts, while the spins of the superpartners differ by  $1/2$  unit. However, spin determinations appear to be difficult at the LHC (or at hadron colliders in general), where the center of mass energy in each event is unknown. In addition, the momenta of the two dark matter candidates in the event are also unknown. Recently it has been suggested that a charge asymmetry in the lepton-jet invariant mass distributions from a particular cascade, can be used to discriminate SUSY from the case of pure phase space decays [9] and is an indirect indication of the superparticle spins. It is therefore natural to ask whether this method can be extended to the case of SUSY versus UED discrimination.

To answer this question, we first choose a study point in UED with  $R^{-1} = 500$  GeV. Then we adjust the relevant MSSM parameters until we get a matching spectrum. Following [9], we concentrate on the cascade decay  $\tilde{q} \rightarrow q\tilde{\chi}_2^0 \rightarrow q\ell^\pm\tilde{\ell}_L^\mp \rightarrow q\ell^+\ell^-\tilde{\chi}_1^0$  in SUSY and the

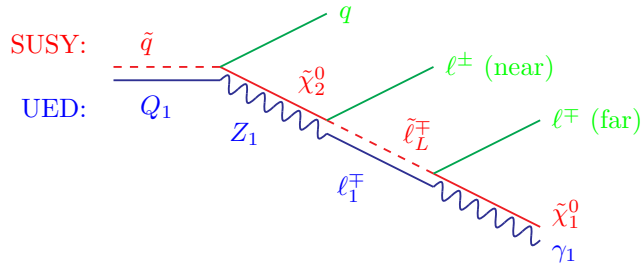


FIG. 10: Twin diagrams in SUSY and UED. The upper (red) line corresponds to the cascade decay  $\tilde{q} \rightarrow q\tilde{\chi}_2^0 \rightarrow q\ell^\pm\tilde{\ell}_L^\mp \rightarrow q\ell^\pm\ell^-\tilde{\chi}_1^0$  in SUSY. The lower (blue) line corresponds to the cascade decay  $Q_1 \rightarrow qZ_1 \rightarrow q\ell^\pm\ell_1^\mp \rightarrow q\ell^\pm\ell^-\gamma_1$  in UED. In either case the observable final state is the same:  $q\ell^+\ell^-\cancel{E}_T$ .

analogous decay chain  $Q_1 \rightarrow qZ_1 \rightarrow q\ell^\pm\ell_1^\mp \rightarrow q\ell^+\ell^-\gamma_1$  in UED [11, 12]. Both of these processes are illustrated in Fig. 10.

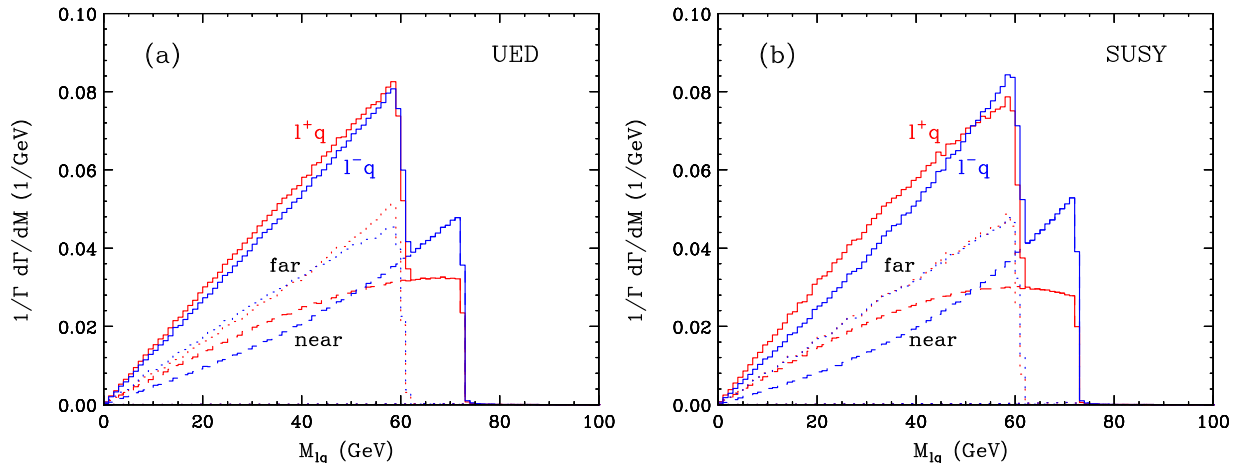


FIG. 11: Lepton-quark invariant mass distributions in (a) UED with  $R^{-1} = 500$  GeV and (b) supersymmetry with a matching sparticle spectrum. We show separately the distributions with the near and far lepton, and their sum. The positive (negative) charge leptons are shown in red (blue).

Next, one forms the lepton-quark invariant mass distributions  $M_{\ell q}$  (see Fig. 11). The spin of the intermediate particle ( $Z_1$  in UED or  $\tilde{\chi}_2^0$  in SUSY) governs the shape of the distributions for the near lepton. However, in practice we cannot distinguish the near and far lepton, and one has to include the invariant mass combinations with both leptons. This tends to wash out the spin correlations, but a residual effect remains, which is due to the

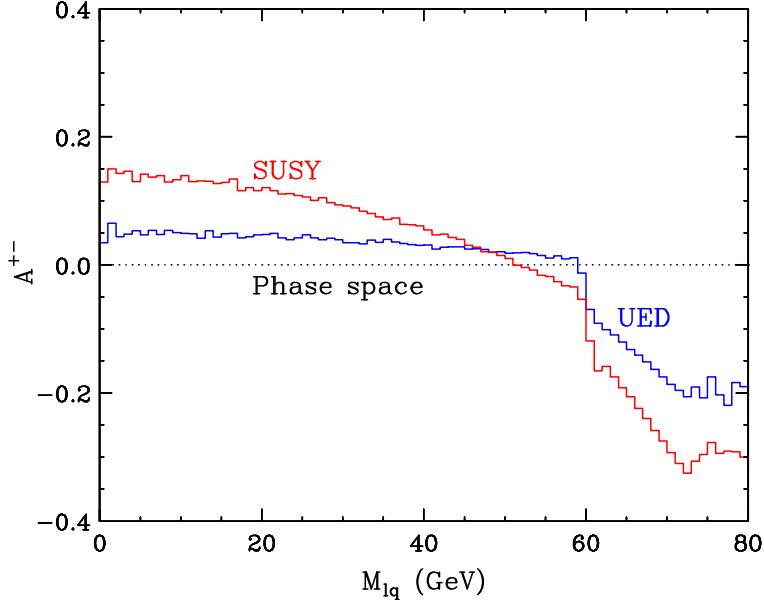


FIG. 12: Comparison of the charge asymmetry  $A^{+-}$  defined in eq. (8) as computed in the case of UED with  $R^{-1} = 500$  GeV and the case of supersymmetry with a matching sparticle spectrum.

different number of quarks and antiquarks in the proton, which in turn leads to a difference in the production cross-sections for squarks and anti-squarks [9]. The spin correlations are encoded in the charge asymmetry [9]

$$A^{+-} \equiv \left( \frac{dN(q\ell^+)}{dM_{ql}} - \frac{dN(q\ell^-)}{dM_{ql}} \right) / \left( \frac{dN(q\ell^+)}{dM_{ql}} + \frac{dN(q\ell^-)}{dM_{ql}} \right), \quad (8)$$

where  $q$  stands for both a quark and an antiquark, and  $N(q\ell^+)$  ( $N(q\ell^-)$ ) is the number of entries with positively (negatively) charged lepton. Our comparison between  $A^{+-}$  in the case of UED and SUSY [11, 12] is shown in Fig. 12. We see that although there is some minor difference in the shape of the asymmetry curves, overall the two cases appear to be very difficult to discriminate unambiguously, especially since the regions near the two ends of the plot, where the deviation is the largest, also happen to suffer from poorest statistics. Notice that we have not included detector effects or backgrounds. Finally, and perhaps most importantly, this analysis ignores the combinatorial background from the other jets in the event, which could be misinterpreted as the starting point of the cascade depicted in Fig. 10. Overall, Fig. 12 shows that although the asymmetry (8) does encode some spin correlations, distinguishing between the specific cases of UED and SUSY appears challenging. These results have been recently confirmed in [14], where in addition the authors considered a study point with larger mass splittings, as expected in typical SUSY models. Under those

circumstances the asymmetry distributions appear to be more distinct than the case shown in Fig. 12, which is a source of optimism. It remains to be seen whether this conclusion persists in a general setting, and once the combinatorial backgrounds are included [69].

## V. CONCLUSIONS

In this paper we have discussed the differences and similarities in the hadron collider phenomenology of models with Universal Extra Dimensions and supersymmetry. We identified the higher level KK modes of UED and the spin quantum numbers of the new particles as the only two reliable discriminators between the two scenarios. We then proceeded to study the discovery reach for level 2 KK modes in UED at hadron colliders. We showed that the  $n = 2$  KK gauge bosons offer the best prospects for detection, in particular the  $\gamma_2$  and  $Z_2$  resonances can be *separately* discovered at the LHC. Is this a proof of UED? Not quite – these resonances could still be interpreted as  $Z'$  gauge bosons, but their close degeneracy is a smoking gun for UED. Furthermore, although we did not show any results to this effect in this paper, it is clear that the  $W_2^\pm$  KK mode can also be looked for and discovered in its decay to SM leptons. One can then measure  $m_{W_2}$  and show that it is very close to  $m_{Z_2}$  and  $m_{\gamma_2}$ , which would further strengthen the case for UED. Unfortunately, the spin discrimination is not so straightforward, and requires further studies. The asymmetry method of Barr seems to fail as a universal discriminator between SUSY and UED, although it rules out the absence of any spin correlations.

While in this paper we only concentrated on the Minimal UED model, it should be kept in mind that there are many interesting possibilities for extending the analysis to a more general setup. For example, non-vanishing boundary terms at the scale  $\Lambda$  can distort the Minimal UED spectrum beyond recognition. A priori, in such a relaxed framework the UED-SUSY confusion can be “complete” in the context of a hadron collider and a preliminary study is under way to address this issue [78]. The UED collider phenomenology is also very different in the case of a “fat” brane [79, 80], charged LKPs [81] or KK graviton superwimps [82, 83]. Notice that Little Higgs models with  $T$ -parity [84, 85, 86] are very similar to UED, and can also be confused with supersymmetry.

## Acknowledgments

We thank H.-C. Cheng and B. Dobrescu for stimulating discussions. AD is supported by the US Department of Energy and the Michigan Center for Theoretical Physics. The work of KK and KM is supported in part by a US Department of Energy Outstanding Junior Investigator award under grant DE-FG02-97ER41209.

- 
- [1] T. Appelquist, H. C. Cheng and B. A. Dobrescu, “Bounds on universal extra dimensions,” *Phys. Rev. D* **64**, 035002 (2001) [arXiv:hep-ph/0012100].
  - [2] H. C. Cheng, K. T. Matchev and M. Schmaltz, “Bosonic supersymmetry? Getting fooled at the LHC,” *Phys. Rev. D* **66**, 056006 (2002) [arXiv:hep-ph/0205314].
  - [3] J. L. Feng, M. E. Peskin, H. Murayama and X. Tata, “Testing supersymmetry at the next linear collider,” *Phys. Rev. D* **52**, 1418 (1995) [arXiv:hep-ph/9502260].
  - [4] M. Battaglia, A. Datta, A. De Roeck, K. Kong and K. T. Matchev, “Contrasting supersymmetry and universal extra dimensions at the CLIC multi-TeV  $e^+ e^-$  collider,” *JHEP* **0507**, 033 (2005) [arXiv:hep-ph/0502041].
  - [5] G. Bhattacharyya, P. Dey, A. Kundu and A. Raychaudhuri, “Probing universal extra dimension at the International Linear Collider,” arXiv:hep-ph/0502031.
  - [6] B. Bhattacharjee and A. Kundu, “The International Linear Collider as a Kaluza-Klein factory,” arXiv:hep-ph/0508170.
  - [7] S. Riemann, “ $Z'$  signals from Kaluza-Klein dark matter,” arXiv:hep-ph/0508136.
  - [8] D. J. H. Chung, L. L. Everett, G. L. Kane, S. F. King, J. Lykken and L. T. Wang, “The soft supersymmetry-breaking Lagrangian: Theory and applications,” *Phys. Rept.* **407**, 1 (2005) [arXiv:hep-ph/0312378].
  - [9] A. J. Barr, “Determining the spin of supersymmetric particles at the LHC using lepton charge asymmetry,” *Phys. Lett. B* **596**, 205 (2004) [arXiv:hep-ph/0405052].
  - [10] K. Kong, talk given at the 2005 International Linear Collider Workshop (LCWS05), Stanford, CA, 18 - 22 March, 2005.
  - [11] K. Matchev, talks given at the APS meeting, Tampa, FL, April 16 and 17, 2005.
  - [12] K. Kong, talk given at the Pheno 2005 Symposium, Madison, WI, May 3, 2005.

- [13] M. Battaglia, A. K. Datta, A. De Roeck, K. Kong and K. T. Matchev, “Contrasting supersymmetry and universal extra dimensions at colliders,” arXiv:hep-ph/0507284.
- [14] J. M. Smillie and B. R. Webber, “Distinguishing Spins in Supersymmetric and Universal Extra Dimension Models at the Large Hadron Collider,” arXiv:hep-ph/0507170.
- [15] B. A. Dobrescu and E. Ponton, “Chiral compactification on a square,” JHEP **0403**, 071 (2004) [arXiv:hep-th/0401032].
- [16] G. Burdman, B. A. Dobrescu and E. Ponton, “Six-dimensional gauge theory on the chiral square,” arXiv:hep-ph/0506334.
- [17] N. Arkani-Hamed, H. C. Cheng, B. A. Dobrescu and L. J. Hall, “Self-breaking of the standard model gauge symmetry,” Phys. Rev. D **62**, 096006 (2000) [arXiv:hep-ph/0006238].
- [18] P. Bucci and B. Grzadkowski, “The effective potential and vacuum stability within universal extra dimensions,” Phys. Rev. D **68**, 124002 (2003) [arXiv:hep-ph/0304121].
- [19] P. Bucci, B. Grzadkowski, Z. Lalak and R. Matyszkiewicz, “Electroweak symmetry breaking and radion stabilization in universal extra dimensions,” JHEP **0404**, 067 (2004) [arXiv:hep-ph/0403012].
- [20] T. Appelquist, B. A. Dobrescu, E. Ponton and H. U. Yee, “Neutrinos vis-a-vis the six-dimensional standard model,” Phys. Rev. D **65**, 105019 (2002) [arXiv:hep-ph/0201131].
- [21] R. N. Mohapatra and A. Perez-Lorenzana, “Neutrino mass, proton decay and dark matter in TeV scale universal extra dimension models,” Phys. Rev. D **67**, 075015 (2003) [arXiv:hep-ph/0212254].
- [22] T. Appelquist, B. A. Dobrescu, E. Ponton and H. U. Yee, “Proton stability in six dimensions,” Phys. Rev. Lett. **87**, 181802 (2001) [arXiv:hep-ph/0107056].
- [23] B. A. Dobrescu and E. Poppitz, “Number of fermion generations derived from anomaly cancellation,” Phys. Rev. Lett. **87**, 031801 (2001) [arXiv:hep-ph/0102010].
- [24] H. Georgi, A. K. Grant and G. Hailu, “Brane couplings from bulk loops,” Phys. Lett. B **506**, 207 (2001) [arXiv:hep-ph/0012379].
- [25] G. von Gersdorff, N. Irges and M. Quiros, “Bulk and brane radiative effects in gauge theories on orbifolds,” Nucl. Phys. B **635**, 127 (2002) [arXiv:hep-th/0204223].
- [26] H. C. Cheng, K. T. Matchev and M. Schmaltz, “Radiative corrections to Kaluza-Klein masses,” Phys. Rev. D **66**, 036005 (2002) [arXiv:hep-ph/0204342].
- [27] K. Agashe, N. G. Deshpande and G. H. Wu, “Can extra dimensions accessible to the SM

- explain the recent measurement of anomalous magnetic moment of the muon?," Phys. Lett. B **511**, 85 (2001) [arXiv:hep-ph/0103235].
- [28] K. Agashe, N. G. Deshpande and G. H. Wu, "Universal extra dimensions and  $b \rightarrow s \gamma$ ," Phys. Lett. B **514**, 309 (2001) [arXiv:hep-ph/0105084].
- [29] T. Appelquist and B. A. Dobrescu, "Universal extra dimensions and the muon magnetic moment," Phys. Lett. B **516**, 85 (2001) [arXiv:hep-ph/0106140].
- [30] F. J. Petriello, "Kaluza-Klein effects on Higgs physics in universal extra dimensions," JHEP **0205**, 003 (2002) [arXiv:hep-ph/0204067].
- [31] T. Appelquist and H. U. Yee, "Universal extra dimensions and the Higgs boson mass," Phys. Rev. D **67**, 055002 (2003) [arXiv:hep-ph/0211023].
- [32] D. Chakraverty, K. Huitu and A. Kundu, "Effects of universal extra dimensions on  $B_0$  - anti- $B_0$  mixing," Phys. Lett. B **558**, 173 (2003) [arXiv:hep-ph/0212047].
- [33] A. J. Buras, M. Spranger and A. Weiler, "The impact of universal extra dimensions on the unitarity triangle and rare K and B decays," Nucl. Phys. B **660**, 225 (2003) [arXiv:hep-ph/0212143].
- [34] J. F. Oliver, J. Papavassiliou and A. Santamaria, "Universal extra dimensions and  $Z \rightarrow b\bar{b}$ ," Phys. Rev. D **67**, 056002 (2003) [arXiv:hep-ph/0212391].
- [35] A. J. Buras, A. Poschenrieder, M. Spranger and A. Weiler, "The impact of universal extra dimensions on  $B \rightarrow X/s \gamma$ ,  $B \rightarrow X/s \text{ gluon}$ ,  $B \rightarrow X/s \mu^+ \mu^-$ ,  $K(L) \rightarrow \pi^0 e^+ e^-$ , and  $\epsilon'/\epsilon$ ," Nucl. Phys. B **678**, 455 (2004) [arXiv:hep-ph/0306158].
- [36] E. O. Iltan, "The  $\mu \rightarrow e\gamma$  and  $\tau \rightarrow \mu\gamma$  decays in the general two Higgs doublet model with the inclusion of one universal extra dimension," JHEP **0402**, 065 (2004) [arXiv:hep-ph/0312311].
- [37] S. Khalil and R. Mohapatra, "Flavor violation and extra dimensions," Nucl. Phys. B **695**, 313 (2004) [arXiv:hep-ph/0402225].
- [38] K. R. Dienes, E. Dudas and T. Gherghetta, "Grand unification at intermediate mass scales through extra dimensions," Nucl. Phys. B **537**, 47 (1999) [arXiv:hep-ph/9806292].
- [39] G. Servant and T. M. Tait, "Is the lightest Kaluza-Klein particle a viable dark matter candidate?" Nucl. Phys. B **650**, 391 (2003) [arXiv:hep-ph/0206071].
- [40] D. Majumdar, "Relic densities for Kaluza-Klein dark matter," Mod. Phys. Lett. A **18**, 1705 (2003).
- [41] M. Kakizaki, S. Matsumoto, Y. Sato and M. Senami, "Significant effects of second KK particles

- on LKP dark matter physics,” *Phys. Rev. D* **71**, 123522 (2005) [arXiv:hep-ph/0502059].
- [42] M. Kakizaki, S. Matsumoto, Y. Sato and M. Senami, “Relic abundance of LKP dark matter in UED model including effects of second KK resonances,” arXiv:hep-ph/0508283.
- [43] F. Burnell and G. D. Kribs, “The abundance of Kaluza-Klein dark matter with coannihilation,” arXiv:hep-ph/0509118.
- [44] K. Kong and K. T. Matchev, “Precise calculation of the relic density of Kaluza-Klein dark matter in universal extra dimensions,” arXiv:hep-ph/0509119.
- [45] H. C. Cheng, J. L. Feng and K. T. Matchev, “Kaluza-Klein dark matter,” *Phys. Rev. Lett.* **89**, 211301 (2002) [arXiv:hep-ph/0207125].
- [46] G. Servant and T. M. Tait, “Elastic scattering and direct detection of Kaluza-Klein dark matter,” *New J. Phys.* **4**, 99 (2002) [arXiv:hep-ph/0209262].
- [47] D. Majumdar, “Detection rates for Kaluza-Klein dark matter,” *Phys. Rev. D* **67**, 095010 (2003) [arXiv:hep-ph/0209277].
- [48] D. Hooper and G. D. Kribs, “Probing Kaluza-Klein dark matter with neutrino telescopes,” *Phys. Rev. D* **67**, 055003 (2003) [arXiv:hep-ph/0208261].
- [49] G. Bertone, G. Servant and G. Sigl, “Indirect detection of Kaluza-Klein dark matter,” *Phys. Rev. D* **68**, 044008 (2003) [arXiv:hep-ph/0211342].
- [50] D. Hooper and G. D. Kribs, “Kaluza-Klein dark matter and the positron excess,” *Phys. Rev. D* **70**, 115004 (2004) [arXiv:hep-ph/0406026].
- [51] L. Bergstrom, T. Bringmann, M. Eriksson and M. Gustafsson, “Gamma rays from Kaluza-Klein dark matter,” *Phys. Rev. Lett.* **94**, 131301 (2005) [arXiv:astro-ph/0410359].
- [52] E. A. Baltz and D. Hooper, “Kaluza-Klein dark matter, electrons and gamma ray telescopes,” *JCAP* **0507**, 001 (2005) [arXiv:hep-ph/0411053].
- [53] L. Bergstrom, T. Bringmann, M. Eriksson and M. Gustafsson, “Two photon annihilation of Kaluza-Klein dark matter,” *JCAP* **0504**, 004 (2005) [arXiv:hep-ph/0412001].
- [54] T. Bringmann, “High-energetic cosmic antiprotons from Kaluza-Klein dark matter,” *JCAP* **0508**, 006 (2005) [arXiv:astro-ph/0506219].
- [55] A. Barrau, P. Salati, G. Servant, F. Donato, J. Grain, D. Maurin and R. Taillet, “Kaluza-Klein dark matter and galactic antiprotons,” arXiv:astro-ph/0506389.
- [56] A. Birkedal, K. T. Matchev, M. Perelstein and A. Spray, “Robust gamma ray signature of WIMP dark matter,” arXiv:hep-ph/0507194.



- [57] H. C. Cheng, “Universal extra dimensions at the e- e- colliders,” *Int. J. Mod. Phys. A* **18**, 2779 (2003) [arXiv:hep-ph/0206035].
- [58] A. Perez-Lorenzana and R. N. Mohapatra, “Effect of extra dimensions on gauge coupling unification,” *Nucl. Phys. B* **559**, 255 (1999) [arXiv:hep-ph/9904504].
- [59] H. C. Cheng, B. A. Dobrescu and C. T. Hill, “Gauge coupling unification with extra dimensions and gravitational scale effects,” *Nucl. Phys. B* **573**, 597 (2000) [arXiv:hep-ph/9906327].
- [60] N. Arkani-Hamed, S. Dimopoulos and G. R. Dvali, “The hierarchy problem and new dimensions at a millimeter,” *Phys. Lett. B* **429**, 263 (1998) [arXiv:hep-ph/9803315].
- [61] G. F. Giudice, R. Rattazzi and J. D. Wells, “Quantum gravity and extra dimensions at high-energy colliders,” *Nucl. Phys. B* **544**, 3 (1999) [arXiv:hep-ph/9811291].
- [62] E. A. Mirabelli, M. Perelstein and M. E. Peskin, “Collider signatures of new large space dimensions,” *Phys. Rev. Lett.* **82**, 2236 (1999) [arXiv:hep-ph/9811337].
- [63] A. Pukhov *et al.*, “CompHEP: A package for evaluation of Feynman diagrams and integration over multi-particle phase space. User’s manual for version 33,” arXiv:hep-ph/9908288.
- [64] T. G. Rizzo, “Probes of universal extra dimensions at colliders,” *Phys. Rev. D* **64**, 095010 (2001) [arXiv:hep-ph/0106336].
- [65] C. Macesanu, C. D. McMullen and S. Nandi, “Collider implications of universal extra dimensions,” *Phys. Rev. D* **66**, 015009 (2002) [arXiv:hep-ph/0201300].
- [66] H. L. Lai *et al.* [CTEQ Collaboration], “Global QCD analysis of parton structure of the nucleon: CTEQ5 parton distributions,” *Eur. Phys. J. C* **12**, 375 (2000) [arXiv:hep-ph/9903282].
- [67] C. D. Carone, J. M. Conroy, M. Sher and I. Turan, “Universal extra dimensions and Kaluza Klein bound states,” *Phys. Rev. D* **69**, 074018 (2004) [arXiv:hep-ph/0312055].
- [68] E. De Pree and M. Sher, “Kaluza-Klein mesons in universal extra dimensions,” arXiv:hep-ph/0507313.
- [69] A. Datta, K. Kong and K. T. Matchev, in preparation.
- [70] M. Carena, A. Daleo, B. A. Dobrescu and T. M. P. Tait, “ $Z'$  gauge bosons at the Tevatron,” *Phys. Rev. D* **70**, 093009 (2004) [arXiv:hep-ph/0408098].
- [71] D. A. Dicus, C. D. McMullen and S. Nandi, “Collider implications of Kaluza-Klein excitations of the gluons,” *Phys. Rev. D* **65**, 076007 (2002) [arXiv:hep-ph/0012259].
- [72] P. Nath, Y. Yamada and M. Yamaguchi, “Probing the nature of compactification with Kaluza-Klein excitations at the Large Hadron Collider,” *Phys. Lett. B* **466**, 100 (1999)

- [arXiv:hep-ph/9905415].
- [73] T. G. Rizzo, “Kaluza-Klein /  $Z'$  differentiation at the LHC and linear collider,” JHEP **0306**, 021 (2003) [arXiv:hep-ph/0305077].
- [74] D. Acosta, private communication.
- [75] D. Bourilkov, talk given at the LPC Muon Meeting, Fermilab, December 2004, <http://bourilko.home.cern.ch/bourilko/dblpcdec04.pdf>.
- [76] T. Sjostrand, L. Lonnblad, S. Mrenna and P. Skands, “PYTHIA 6.3: Physics and manual,” arXiv:hep-ph/0308153.
- [77] R. Blair *et al.* [CDF-II Collaboration], “The CDF-II detector: Technical design report,” preprint FERMILAB-PUB-96-390-E.
- [78] A. Datta, G. L. Kane and M. Toharia, to appear.
- [79] C. Macesanu, C. D. McMullen and S. Nandi, “New signal for universal extra dimensions,” Phys. Lett. B **546**, 253 (2002) [arXiv:hep-ph/0207269].
- [80] C. Macesanu, S. Nandi and M. Rujoiu, “Single Kaluza Klein production in universal extra dimensions,” Phys. Rev. D **71**, 036003 (2005) [arXiv:hep-ph/0407253].
- [81] M. Byrne, “Universal extra dimensions and charged LKPs,” Phys. Lett. B **583**, 309 (2004) [arXiv:hep-ph/0311160].
- [82] J. L. Feng, A. Rajaraman and F. Takayama, “Superweakly-interacting massive particles,” Phys. Rev. Lett. **91**, 011302 (2003) [arXiv:hep-ph/0302215].
- [83] J. L. Feng, S. Su and F. Takayama, “Guaranteed rates for dark matter production at the Large Hadron Collider and International Linear Collider,” arXiv:hep-ph/0503117.
- [84] H. C. Cheng and I. Low, “TeV symmetry and the little hierarchy problem,” JHEP **0309**, 051 (2003) [arXiv:hep-ph/0308199].
- [85] H. C. Cheng and I. Low, “Little hierarchy, little Higgses, and a little symmetry,” JHEP **0408**, 061 (2004) [arXiv:hep-ph/0405243].
- [86] J. Hubisz and P. Meade, “Phenomenology of the littlest Higgs with T-parity,” Phys. Rev. D **71**, 035016 (2005) [arXiv:hep-ph/0411264].